Smoke radiocarbon measurements from Indonesian fires provide evidence for burning of millennia-aged peat

Elizabeth B. Wiggins[a,1], Claudia I. Czimczik[a], Guaciara M. Santos[a], Yang Chen[a], Xiaomei Xu[a], Sandra R. Holden[a], James T. Randerson[a,1], Charles F. Harvey[b,c], Fuu Ming Kai[b,2], and Liya E. Yu[d,e]

[a]Department of Earth System Science, University of California, Irvine, CA 92697; [b]Center for Environmental Sensing and Modeling, Singapore-MIT Alliance for Research and Technology, 138602 Singapore; [c]Parsons Laboratory, Department of Civil and Environmental Engineering, Massachusetts Institute of Technology, Cambridge, MA, 02139; [d]Department of Civil & Environmental Engineering, National University of Singapore, 119260 Singapore; and [e]National University of Singapore Environmental Research Institute, National University of Singapore, 119260 Singapore

In response to a strong El Niño, fires in Indonesia during September and October 2015 released a large amount of carbon dioxide and created a massive regional smoke cloud that severely degraded air quality in many urban centers across Southeast Asia. Although several lines of evidence indicate that peat burning was a dominant contributor to emissions in the region, El Niño-induced drought is also known to increase deforestation fires and agricultural waste burning in plantations. As a result, uncertainties remain with respect to partitioning emissions among different ecosystem and fire types. Here we measured the radiocarbon content (^{14}C) of carbonaceous aerosol samples collected in Singapore from September 2014 through October 2015, with the aim of identifying the age and origin of fire-emitted fine particulate matter (particulate matter with an aerodynamic diameter less than or equal to 2.5 μm). The Δ^{14}C of fire-emitted aerosol was -76 ± 51‰, corresponding to a carbon pool of combusted organic matter with a mean turnover time of 800 ± 420 y. Our observations indicated that smoke plumes reaching Singapore originated primarily from peat burning (~85%), and not from deforestation fires or waste burning. Atmospheric transport modeling confirmed that fires in Sumatra and Borneo were dominant contributors to elevated $PM_{2.5}$ in Singapore during the fire season. The mean age of the carbonaceous aerosol, which predates the Industrial Revolution, highlights the importance of improving peatland fire management during future El Niño events for meeting climate mitigation and air quality commitments.

tropical peatlands | global carbon cycle | human health | isotope | land cover change

During 2015, Indonesia experienced an exceptionally intense September–October fire season fueled by El Niño-induced drought. Emissions from the fires were substantial, increasing CO_2 and CH_4 in the global atmosphere. Greenhouse gas emissions estimates derived from both land surface and atmospheric remote sensing observations indicate that the fires emitted between 0.89 and 1.5 Pg CO_2-Eq. (1–5), which is the largest regional source since the strong 1997–1998 El Niño (1, 3, 6, 7) and is equivalent to about 20% of the 1 ppm positive CO_2 anomaly observed at Mauna Loa during 2015 (8). Prevailing winds transported aerosols from the Indonesian fires to population centers across the Maritime Continent, reducing air quality in many cities and affecting the health of more than 40 million people (9). Widespread burning from escaped fires across Sumatra, Kalimantan, and West Papua degraded critical habitat for endangered plant and animal species, including orangutans and Sumatran tigers (10). Together, the climate, human health, and ecosystem damages from the fires were substantial and widely distributed among stakeholders and regional communities (11–13). This contrasts with the benefits accrued to the agricultural sector from land clearing and peatland drainage. Lowering the water table increases agricultural yield by drying near-surface peat, but also makes peatlands flammable. The costs

and benefits of these land use practices operate on different spatial and temporal scales, making it difficult to design effective policy and management solutions (13).

The extreme 2015 fire season was a part of a broader set of climate–human–ecosystem interactions across the Maritime Continent that have been evolving over a period of decades from rapid changes in land use (14). These interactions are unique because of the widespread distribution of tropical peatlands in low-elevation areas that have been intensively deforested, drained, and further modified to support agricultural production, rendering them vulnerable to anthropogenic fire. Loss of forest cover in peatlands has been extensive during the last several decades, declining by 71% across Peninsular Malaysia, Sumatra, and Borneo between 1990 and 2015 (15). Peatland soils store between 28 and 57 Pg C in Indonesia alone, and far exceed aboveground carbon stocks (16, 17). The vulnerability of peat to fire increases considerably with canal construction, used for timber extraction and plantation development (18, 19), with drainage efforts undertaken by both large-scale industrial operators and smallholder farmers (20). Tropical peat surface layers become flammable when the water table declines (21). Upon ignition, peat fires can persist for long periods at relatively low

Significance

We report radiocarbon (^{14}C) measurements of carbonaceous aerosol originating from fires on the islands of Sumatra and Borneo. These data provide information about what types of ecosystems burned and are critical for linking the human health effects of fires to the anthropogenic build-up of atmospheric CO_2. Our measurements confirm that peat emissions were the dominant source of aerosols in Singapore during the 2015 El Niño and provide a means for monitoring the success of policies designed to protect peatland areas during future drought events.

ENVIRONMENTAL SCIENCES

temperatures and oxygen levels (6, 22). As a consequence of smoldering combustion, peat fires emit three or more times the amount of particulate matter with an aerodynamic diameter less than or equal to 2.5 µm ($PM_{2.5}$) released by deforestation fires per kilogram of fuel consumed (23–26). Belowground burning can also make it difficult to accurately detect and quantify emissions using optical and thermal remote sensing techniques because of smaller postfire surface reflectance changes, shielding of the surface by regional smoke plumes and haze, and smaller thermal radiance anomalies (5). Burning in deep layers of accumulated peat modifies regional greenhouse gas budgets and indicates these ecosystems no longer operate as a slow, sustained sink in the global carbon cycle (27, 28).

Although peatland burning is well established as an important source of fire emissions during drought events in Indonesia, uncertainties remain with respect to contributions from different ecosystem and land use activities. Page et al. (6) estimated that between 0.81 and 2.57 Gt C, or 79–84% of total carbon (TC) emissions, were released from fires in drained peatlands across Indonesia during the 1997–1998 El Niño. For more recent El Niño events, and with the availability of higher-quality satellite observations, nonpeatland fires have been identified as an important emissions source. Marlier et al. (29), for example, estimated that 38% of carbon emissions from forest concessions on Sumatra originated from nonpeatland ecosystem types during the 2006 El Niño. Using high-resolution synthetic aperture radar data from the Sentinel 1B satellite, Lohberger et al. (5) estimated that emissions from peat accounted for only 33–45% of carbon emissions released by fires during the 2015 El Niño on Sumatra, Borneo, and Papua New Guinea. The relatively small fraction of peat emissions in this study originates from the application of lower fuel consumption rates in degraded peatlands (19) and near-complete combustion of aboveground biomass from primary and secondary forests. The Lohberger et al. (5) budget contrasts with other satellite remote sensing analyses that provide evidence for a more prominent role of peat as a source for emissions and fire activity during the 2015 fire season (1, 30, 31). The differences in these emissions estimates highlight the need to develop independent constraints on the attribution of emissions among different land cover types and among above- and belowground carbon pools.

Radiocarbon (^{14}C) measurements of carbonaceous aerosols may provide independent information about the contribution of peat burning to regional fire emissions budgets, complementing satellite remote sensing and in situ field measurements. The isotopic constraint comes from a unique ^{14}C labeling of terrestrial biomass that has occurred during the last 60 y as a consequence of aboveground nuclear weapons testing (32). The flow of this bomb-derived ^{14}C through plant, litter, and soil organic matter pools enables the diagnosis of carbon turnover times on timescales of years to decades for ecosystem (33) and aerosol samples (34). For soil organic matter and other biomass formed before the bomb era, radioactive decay of ^{14}C provides additional information about carbon ages over timescales of centuries to millennia (35). In the context of tracing the origin of smoke from Indonesian fires, carbonaceous aerosol originating from the combustion of aboveground biomass, as expected for emissions from deforestation fires or agricultural waste burning in plantations, should be bomb-labeled. Using isotope definitions from Stuiver and Polach (36), this means the $\Delta^{14}C$ should be above the contemporary level observed for atmospheric CO_2 (25 ± 3‰ in 2015). In contrast, carbonaceous aerosol from older peat should have a negative $\Delta^{14}C$, reflecting the longer-term cumulative effects of radioactive decay in organic carbon layers deposited over a period of centuries or millennia (35, 37–43).

Here we report ^{14}C measurements of carbonaceous aerosols from Singapore during the 2014 and 2015 fire seasons, along with carbon concentration observations. Additional measurements from background (low-fire) periods were used to remove the influence of

urban emissions and isolate the carbon isotopic composition of fire-derived aerosol. We use this information to estimate the mean age of the combusted organic material and to distinguish among agricultural waste burning, deforestation, and peat sources. Satellite active fire observations and simulations from the Goddard Earth Observing System Chemical Transport Model (GEOS-Chem) provided a means to identify the contribution of emissions from key source sectors and regions to our aerosol observations.

Results

During September and October 2015, the highest densities of active fires detected by satellite sensors were observed in South Sumatra and in the Central Kalimantan province on Borneo (Fig. 1). During this period, weekly carbonaceous aerosol samples in Singapore had a mean concentration of 67.4 ± 29.6 µg C m^{-3}, or approximately six times higher than urban background levels measured between January and July (Fig. 2A and *SI Appendix*, Table S1). The mean $\Delta^{14}C$ of these samples was −136 ± 57‰, which was considerably elevated compared with the mean of the urban background (−578 ± 78‰; Fig. 2B). Intervals with elevated carbonaceous aerosols in Singapore were synchronized
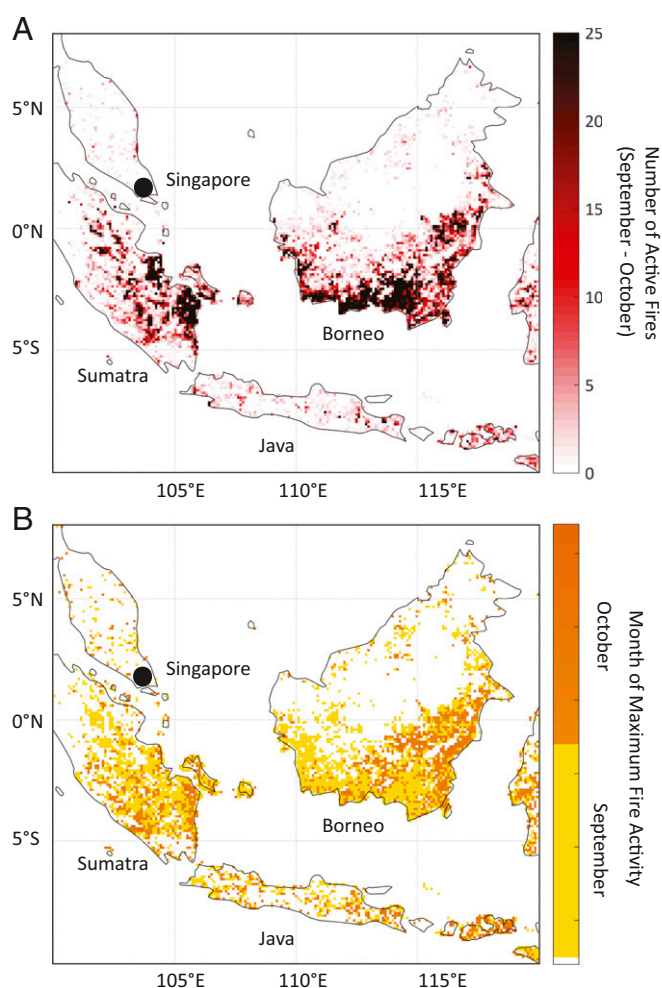
Fig. 1. Location (*A*) and timing (*B*) of satellite-detected active fires during the 2015 September–October fire season across the Maritime Continent. The satellite detections of active fires were from the Moderate Resolution Imaging Spectroradiometer MCD14ML product that combines fire detections from NASA's Aqua and Terra satellites. The units of *A* are number of fire detections per 0.1° grid cell. The month with the maximum number of fire detections in each grid cell is shown in *B*.
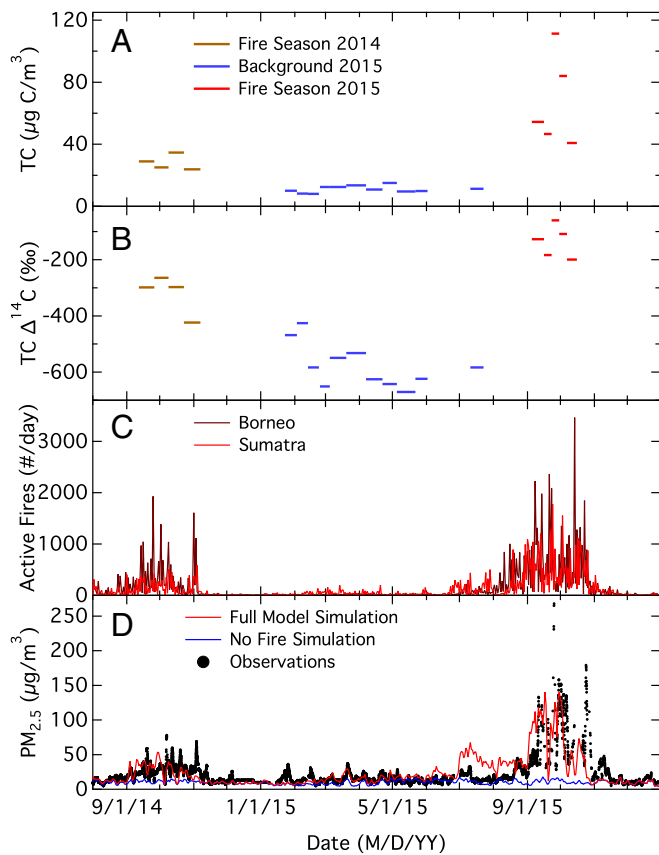
**Fig. 2.** Time series of aerosol composition and fire activity during the 2014 and 2015 fire seasons. (*A*) TC concentration of aerosol samples collected in Singapore during 2014 and 2015. Samples collected during the 2014 fire season are shown in brown, those collected during a low-fire urban background interval during the first half of 2015 are shown in blue, and those collected during the 2015 fire season are shown in red. (*B*) The radiocarbon content [$\Delta^{14}C$; with units of per mil (‰)] of the carbonaceous aerosol shown in *A*. (*C*) The number of satellite active fire detections on the islands of Borneo (dark red) and Sumatra (red). (*D*) PM$_{2.5}$ estimates from the GEOS-Chem atmospheric model with all sources (full; red line) and a model simulation in which fire emissions were excluded (no fire; blue line). Daily average PM$_{2.5}$ observations collected from a site at the National University of Singapore are shown in *D* with black circles.

with high numbers of satellite active fire detections on Borneo and Sumatra (Fig. 2*C*). Atmospheric model simulations with GEOS-Chem indicated fires accounted for more than 80% of the total PM$_{2.5}$ observed in Singapore during September and October 2015 (Fig. 2*D*). Sumatra was the most important source region, accounting for 73% of the total PM$_{2.5}$ derived from fires. Within Sumatra, emissions from the Global Fire Emissions Database version 4s (GFED4s) (31) were highest in southern coastal provinces (e.g., Fig. 1), where there was considerable burning in degraded peatland forests and escaped fires in an industrial pulpwood plantation (30). Borneo accounted for another 18% of the fire aerosol reaching Singapore (*SI Appendix*, Table S2).

During the previous fire season in 2014, a weaker El Niño (44) (*SI Appendix*, Fig. S1) triggered a similar, but smaller, change in aerosol concentration and isotopic composition. Carbonaceous aerosol samples during September and October 2014 had a mean concentration of 28.1 ± 4.9 µg C m^{-3}, which is more than 2.5 times higher than measurements from the subsequent background period. The $\Delta^{14}C$ of these samples (−321 ± 70‰) also was elevated compared with the urban background, but by a lesser degree than during the 2015 fire season. Satellite observations from 2014

showed much lower levels of burning across most of Sumatra and many coastal areas of southern Borneo (*SI Appendix*, Fig. S2), whereas the atmospheric modeling simulations indicated Borneo fire emissions were a proportionally larger component of the total fire signal observed in Singapore during this period (*SI Appendix*, Table S2). Together, the aerosol observations, satellite measurements, and atmospheric model simulations indicated that fire emissions played a smaller, but important, role in modifying PM$_{2.5}$ in Singapore during September and October 2014.

We estimated the $\Delta^{14}C$ of fire-emitted carbonaceous aerosol using a Keeling plot approach (34, 45) to separate urban background contributions from our weekly observations collected during the 2014 and 2015 fire seasons (Fig. 3*A*). From this approach, we estimated that fire-emitted carbonaceous aerosols during 2014 and 2015 had a mean $\Delta^{14}C$ of −76 ± 51‰ (Fig. 3*A*). This estimate was similar to the mean derived from isotope mass balance (Fig. 4*A*). The relatively large uncertainty associated with this estimate likely originated from temporal variation in the location and source of fire emissions during the two fire seasons, as
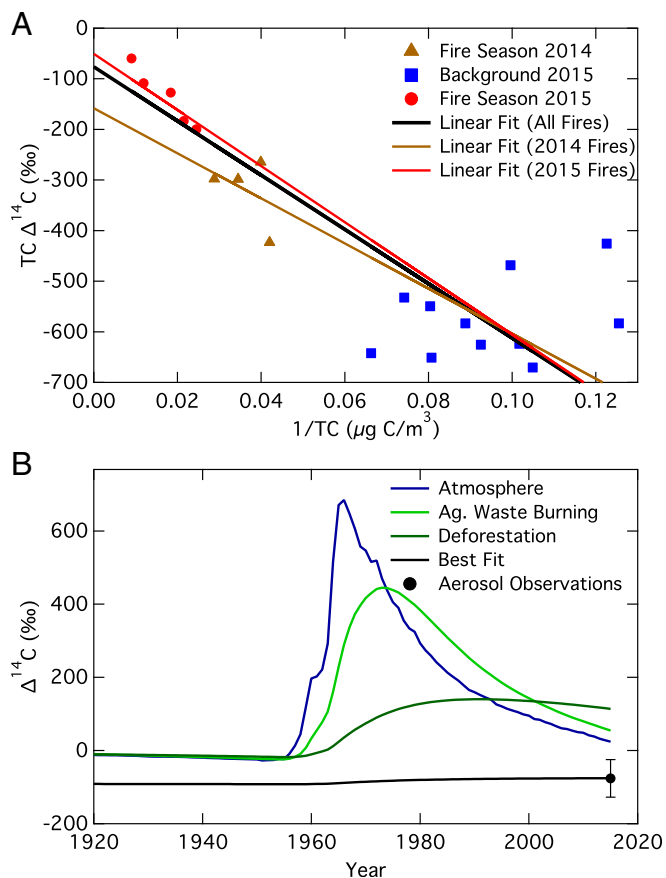

Fig. 3. (*A*) A Keeling plot showing radiocarbon content ($\Delta^{14}C$) vs. the reciprocal of aerosol TC concentration (1/TC). A best-fit line derived from a model II regression, taking into account uncertainty in both $\Delta^{14}C$ and concentration, is shown in black for all of the fire season data from 2014 and 2015. The y intercept for this regression is −76 ± 51‰ and represents the isotopic composition of the fire-emitted aerosol. Brown and red lines denote the best-fit lines for the 2014 and 2015 fire seasons, respectively. *B* shows the $\Delta^{14}C$ of atmospheric CO$_2$ (blue line) and model estimates of agricultural waste burning emissions (light green line) and deforestation (dark green line). A source with a turnover time of 800 ± 420 y (black line) was required to match the observed $\Delta^{14}C$ of the fire-emitted aerosols (black circle). The error bar on the fire-emitted aerosol in *B* denotes 1 SD and was derived from the All Fires regression line shown in *A*.
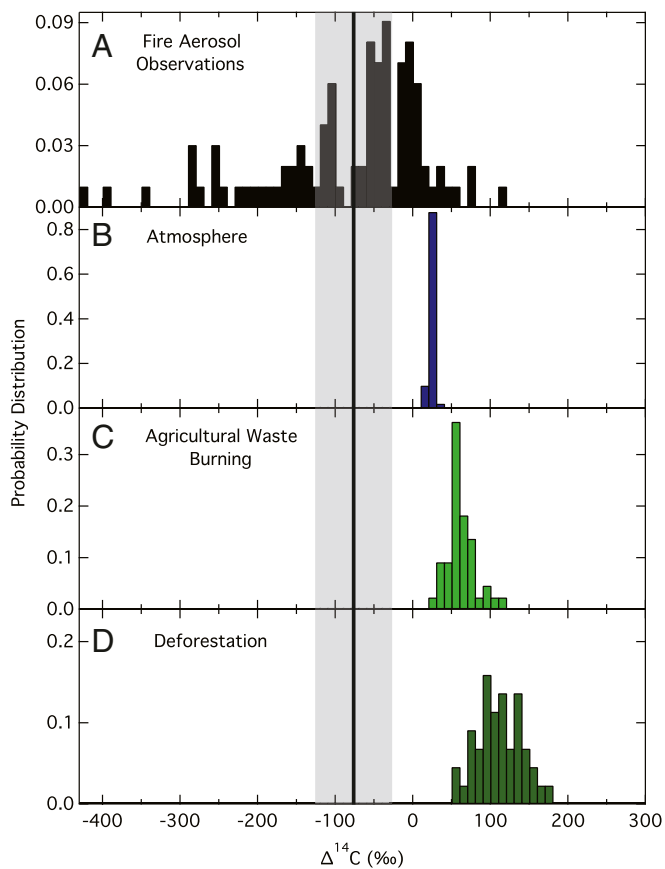
Fig. 4. (A) Histogram of the radiocarbon content (Δ^{14}C) of fire-derived carbonaceous aerosols, using a mass balance approach using all of the aerosol observations from 2014 and 2015. (B) Histogram of Δ^{14}C value of the 2014–2015 atmosphere, using a Monte-Carlo approach with a mean of $25 \pm 3‰$. (C) Histogram of Δ^{14}C values of agricultural waste burning, using a Monte-Carlo approach with a mean of $55 \pm 21‰$, corresponding to a carbon pool with a turnover time of 7.5 ± 4 y. (D) Histogram of Δ^{14}C values of deforestation related fires, using a Monte-Carlo approach with a mean of $114 \pm 26‰$ corresponding to a carbon pool with a turnover time of 55 ± 28 y. The vertical black line and gray shaded area represents the mean and SD of the fire-derived carbonaceous aerosol derived from the Keeling plot approach.

well as variability in the samples used to estimate the concentration and isotopic composition of the urban background.

Using Keeling plots to separate the Δ^{14}C of the fire-emitted carbonaceous aerosol for the different years, we found that the 2014 fire season had a more negative Δ^{14}C ($-158 \pm 87‰$) than the 2015 fire season ($-51 \pm 69‰$). The Δ^{14}C estimate of fire aerosol from 2014 was more uncertain because of the smaller positive concentration anomalies during the fire season, making it more difficult to separate the fire aerosol component from the background. An independent set of 11 daily aerosol filters collected during the 2015 fire season (and obtained using a separate sampling protocol; *SI Appendix*, Fig. S3) also had a more positive isotopic value of the fire end member that was within the uncertainty range of the estimate derived from the 2015 weekly samples.

Our estimate of the mean Δ^{14}C of the fire-emitted carbonaceous aerosol during the 2014 and 2015 fire seasons was significantly lower than atmospheric levels ($-76 \pm 51‰$ vs. $25 \pm 3‰$; $P < 0.01$, using a Student's t test on the data shown in Fig. 4 *A* and *B*). Given the elevated Δ^{14}C of atmospheric CO_2 during the last 60 y from nuclear weapons testing (46), the negative Δ^{14}C of the fire aerosol provided evidence that most of the combusted organic matter was fixed during photosynthesis before the 20th century. Using a simple carbon cycle model to fit the Δ^{14}C

aerosol observations, we estimated that the mean turnover time of the combusted carbon was 800 ± 420 y (Fig. 3*B*).

To help interpret the aerosol observations, we also used a carbon cycle model to estimate the Δ^{14}C of fire aerosols if they originated solely from agricultural waste burning or deforestation (Fig. 4 *C* and *D*). For agricultural waste burning in plantations with an estimated turnover time of 7.5 ± 4 y (47, 48), the expected Δ^{14}C in 2015 would have been $52 \pm 17‰$ (Fig. 4*C*). Similarly, for combustion of forest biomass stocks with an estimated turnover time of 55 ± 28 y (49, 50), the expected Δ^{14}C in 2015 would have been $114 \pm 26‰$ (Fig. 4*D*). The significant difference in the simulated Δ^{14}C distributions for the two aboveground biomass burning sources compared with the aerosol observations shown in Fig. 4*A* provided independent confirmation that deforestation and agricultural waste burning were unlikely to be important contributors to the carbonaceous aerosol we measured in Singapore (Fig. 4).

Discussion

The Δ^{14}C of the fire-emitted carbonaceous aerosol, along with previous work documenting the Δ^{14}C of organic soil profiles in peatlands (35, 37, 39–43, 51–54), indicated that most of the fire aerosol we measured in Singapore originated from the burning of peat. Specifically, the mean turnover time of combusted carbon (800 ± 420 y) allowed for only a small fraction of the aerosol to originate from decadal-scale vegetation pools (49, 50) or surface organic soil layers enriched in ^{14}C atoms from aboveground nuclear weapons testing. A larger fraction of aerosol emissions from aboveground vegetation would have pushed the Δ^{14}C of fire-emitted aerosols above atmospheric levels (Fig. 4).

Uncertainties in our turnover time estimate were consistent with the combustion of peat from a variety of sources and with a broad spectrum of ages. Key processes that likely influenced the Δ^{14}C of the fire aerosol were the amount of burning in degraded peatlands (19), as prior burns and peat oxidation would strip away the acrotelm and bomb-labeled carbon in surface layers; spatial and temporal variations in the depth of the water table that influence the depth of burn (19); the magnitude and spatial pattern of peat oxidation (20); burning location on peat domes relative to the centripetal pattern of decreasing peat age toward the dome center (42); and regional variations in the age structure (and thus Δ^{14}C) of peat profiles (51). Together, these processes were likely important drivers of the large variability in our estimates of fire-aerosol Δ^{14}C (Fig. 4*A*). Because age profiles in peat usually increase monotonically with depth (*SI Appendix*, Fig. S4), to generate smoke with a mean turnover time of 800 ± 420 y, a substantial amount of burning had to originate from peat layers that were older than 1,000 y.

Aerosol Δ^{14}C measurements may provide quantitative constraints on the composition of sources contributing to TC emissions from fires when these observations are combined with emission factors and peat Δ^{14}C profiles. For example, if we assume that peat emissions originated from the top meter of the profile (19) with a mean Δ^{14}C of $-109‰$ (*SI Appendix*, Fig. S4), and that deforestation fires had a mean Δ^{14}C of $114‰$ (Fig. 4*D*), then about $85 \pm 21\%$ of fire aerosol emissions originated from peat, based on a Monte Carlo analysis. This estimate is somewhat higher than the 61–72% estimate of the peat contribution to the fire aerosol load we obtained by combining the fire emissions budget from Lohberger et al. (5), with recent OC emission factors (23, 24) (*SI Appendix*, Table S3). The ^{14}C-based estimate is also somewhat higher than the peat fraction of organic carbon aerosol emissions from GFED4s inventory (*SI Appendix*, Fig. S5 and Table S4), which relies on older (and lower) organic carbon aerosol emission factors (31). We note that uncertainties remain considerable with respect to appropriate regional-scale estimates of emission factors and estimates of isotopic composition of combusted peat, and thus, both the Lohberger et al. (5) and GFED4s (31) estimates of the peat

Wiggins et al.

fraction of carbon emissions are within the range of the lower bound of the observational uncertainty. Nevertheless, the aerosol ^{14}C measurements presented here provide an independent constraint on source attribution that complements remote sensing observations and highlights the critical importance of burning in peatland soils as a driver of El Niño smoke clouds.

Our measurements suggest that systematic regional monitoring of Δ^{14}C in aerosols and trace gases (CO and CH$_4$) during future El Niño events may provide insight about the success of mitigation policy. Policies that are successful in limiting peatland fires (11, 55) should simultaneously lower organic carbon aerosol concentrations and raise the Δ^{14}C of these aerosols. Emission factors of CO, CH$_4$, and organic carbon aerosols should also decline (23–25), highlighting the additional benefits for air quality and the added value accrued from simultaneously measuring CO$_2$ and other trace gas anomalies at remote sites near vulnerable regions (1). Without improvements in land management and peatland conservation, we hypothesize that the Δ^{14}C of regional fire emissions during future El Niño events will decrease over the next several decades as lowering water tables expose older peat layers to decomposition and combustion.

The Δ^{14}C of fire-emitted aerosol during the 2014 fire season was more negative than during the 2015 fire season, suggesting different land areas with older peat layers were subject to combustion. If fires were confined to the same areas each year, the reverse would have occurred: the Δ^{14}C in 2014 would have been more positive because peat deposits are age stratified, and shallower peat, higher in Δ^{14}C, would have burned off first. One possible explanation for the year-to-year difference in Δ^{14}C relates to the strength of El Niño, which was weaker in 2014 (*SI Appendix*, Fig. S1). As a consequence, more burning in peatlands in 2014 may have been confined to areas near canal networks and regions that had previously undergone some degradation (53, 56) (*SI Appendix*, Fig. S2). Analysis of aircraft light detection and ranging observations from Central Kalimantan shows that peatland fires burn more frequently (and thus deeper) in better-drained areas near the banks of canals (19). As a result, combusted organic material in 2014 may have originated from deeper and older peat layers (relative to the original surface before disturbance) that were depleted in ^{14}C. In contrast, during the very strong El Niño in 2015, a lower regional water table may have increased the vulnerability of more pristine areas that had intact aboveground and surface peat carbon pools with stronger labeling from bomb ^{14}C. Burning from these areas with high Δ^{14}C may have more than offset emissions of lower Δ^{14}C aerosols originating from burning near canals and other areas where previous land use had degraded surface peat layers.

The lower Δ^{14}C of fire aerosols in 2014 may also be tied to shifts in emissions contributions from Sumatra and Borneo. In 2014, Borneo had a higher proportion of total active fire detections (Fig. 2C) and contributed to a higher percentage of the fire PM$_{2.5}$ observed in Singapore (*SI Appendix*, Table S2). In some areas of Central Kalimantan, peat slowed or stopped accumulating in the mid- to late Holocene (51), yielding older peat layers near the surface (*SI Appendix*, Fig. S4). Burning appeared more concentrated in these areas (*SI Appendix*, Fig. S2), including areas previously degraded from canal building and fires (53), and thus may have generated smoke with more negative Δ^{14}C. A more quantitative separation of smoke ages from different islands may be possible in future work, but will require a regional network of aerosol sampling, use of a higher-resolution atmospheric model, and a spatially explicit model of peat ages and recent surface losses.

Here we report regionally integrated estimates of the ^{14}C content of smoke originating from Indonesian fires during moderate and extreme El Niño events. Our results indicated that the dominant source of carbonaceous aerosols during the 2014 and 2015 fire seasons was Holocene peat from Sumatra and Borneo. Our measurements confirm that Indonesian fires are predominantly releasing CO$_2$ to the atmosphere that has been out of contact with the atmosphere for centuries and millennia, and thus represent a net perturbation to the global carbon budget. The observations call into question recent fire budgets that suggest a significant amount of emissions originate from aboveground biomass pools or nonpeatland land cover types. Systematic long-term monitoring of ^{14}C content of fire aerosols in the future may be useful for evaluating the effectiveness of mitigation policies designed to protect existing peatland areas, particularly at an integrated province-to-country spatial scale. Together with other recent work, our study highlights the critical dual importance of reducing tropical peatland fires for air quality and climate change mitigation.

Materials and Methods

We collected weekly air samples of PM$_{2.5}$ at the National University of Singapore (1° 17′ 56.65″N, 103° 46′ 16.62″E). Our sampling program spanned the September–October fire seasons of 2014 and 2015, when PM$_{2.5}$ was elevated in Singapore compared with other background (low fire) periods. We defined the fire season for the purpose of this analysis as 1 September–31 October, including any samples that were initiated during this period.

Weekly samples were collected using a light-scattering photometer (ADR1500; Thermo Scientific) on circular 37-mm-diameter quartz microfiber filters (Pallflex Membrane) over intervals of 7–18 d with a flow rate of 0.0912 m^3 air/h. Additional daily samples were collected with a custom-built sharp-cut cyclone (URG) on circular 47-mm-diameter quartz microfiber filters (Pallflex Membrane). All PM$_{2.5}$ samples were analyzed for their ^{14}C and TC content at the W. M. Keck Carbon Cycle Accelerator Mass Spectrometry Facility at the University of California, Irvine (*SI Appendix*, SM1. Aerosol Collection and Analysis and Table S1).

We used two different approaches to separate fire and background components of the TC aerosol samples. First, we used a Keeling plot to compute the y axis intercept (the fire end member) from a regression of Δ^{14}C versus the reciprocal of aerosol concentration. We constructed the regression using all the weekly aerosol samples during 2014 and 2015 (*SI Appendix*, SM2. Quantifying Fire Contributions to TC Aerosol and Eq. S1). Second, we removed the contribution of nonfire aerosol, using isotope mass balance with the concentration and ^{14}C content of individual samples collected during a separate background period when regional fire emissions across the Maritime Continent were low (*SI Appendix*, SM2. Quantifying Fire Contributions to TC Aerosol and Eq. S2).

We used a simple steady-state one-box model with the observed atmospheric history of Δ^{14}C (46, 57) to estimate the turnover time of the combusted carbon that formed the fire-emitted carbonaceous aerosol. We averaged the Δ^{14}C time series for northern and southern tropical regions from Hua et al. (46) to create a mean time series of atmospheric composition for our equatorial study region for the years from 1950 to 2009. We used observations from Barrow, Alaska, to extend the time series from 2009 through 2015, after adjusting this time series with the mean difference (7.2 ± 2.4‰) observed between the Hua et al. (46) time series and the Barrow time series during a period of overlap between 2003 and 2009 (*SI Appendix*, SM3. Radiocarbon Box Model).

To quantify the spatial and temporal variability of active fires on Borneo and Sumatra, we used active fire/thermal anomaly detections from the Moderate Resolution Imaging Spectroradiometer on NASA's Aqua and Terra satellites (58). These observations had a 1.1-km nadir resolution and were processed at the University of Maryland (Collection 5.1; MCD14ML).

We used the GEOS-Chem global 3-D Chemical Transport Model (version 10–01, www.geos-chem.org) to simulate the atmospheric transport of aerosols emitted by fires and other sources. The model was forced with archived GEOS-FP meteorological fields for 2014–2015, which had a temporal resolution of 6 h (3 h for surface variables and mixing depths), a horizontal resolution degraded to 2° (latitude) × 2.5° (longitude), and 72 vertical layers between the surface and 0.01 hPa. We performed aerosol-only simulations using monthly mean OH, NO$_3$, and O$_3$ and total nitrate concentrations archived from a previous full-chemistry simulation. Inputs of aerosol emissions to the model included anthropogenic, biofuel, landscape fire, and natural sources (59) and were managed by the Harvard-NASA Emissions Component (60). GEOS-Chem used GFED4s emissions (31), which were separated into different chemical species within the model, using emission factors for six different fire types, including peat fires and deforestation fires, with the emission factors derived mostly from Akagi et al. (26). Four sets of fire emissions from GFED4s were used in this study. A FULL simulation included

all GFED4s emissions, and in three other simulations, GFED4s emissions were sequentially turned off over Borneo, Sumatra, and all other source regions.

1. Huijnen V, et al. (2016) Fire carbon emissions over maritime Southeast Asia in 2015 largest since 1997. *Sci Rep* 6:26886.
2. Liu J, et al. (2017) Contrasting carbon cycle responses of the tropical continents to the 2015-2016 El Niño. *Science* 358:eaam5690.
3. Field RD, et al. (2016) Indonesian fire activity and smoke pollution in 2015 show persistent nonlinear sensitivity to El Niño-induced drought. *Proc Natl Acad Sci USA* 113:9204–9209.
4. Heymann J, et al. (2017) CO_2 emission of Indonesian fires in 2015 estimated from satellite-derived atmospheric CO_2 concentrations. *Geophys Res Lett* 44:1537–1544.
5. Lohberger S, Stängel M, Atwood EC, Siegert F (2018) Spatial evaluation of Indonesia's 2015 fire-affected area and estimated carbon emissions using Sentinel-1. *Glob Change Biol* 24:644–654.
6. Page SE, et al. (2002) The amount of carbon released from peat and forest fires in Indonesia during 1997. *Nature* 420:61–65.
7. Heil A, Langmann B, Aldrian E (2007) Indonesian peat and vegetation fire emissions: Study on factors influencing large-scale smoke haze pollution using a regional atmospheric chemistry model. *Mitig Adapt Strateg Glob Chang* 12:113–133.
8. Betts RA, Jones CD, Knight JR, Keeling RF, Kennedy JJ (2016) El Niño and a record CO_2 rise. *Nat Clim Chang* 6:806–810.
9. Koplitz SN, et al. (2016) Public health impacts of the severe haze in equatorial Asia in september–october 2015: Demonstration of a new framework for informing fire management strategies to reduce downwind smoke exposure. *Environ Res Lett* 11: 094023.
10. Posa MRC, Wijedasa LS, Corlett RT (2011) Biodiversity and conservation of tropical peat swamp forests. *Bioscience* 61:49–57.
11. Chisholm RA, Wijedasa LS, Swinfield T (2016) The need for long-term remedies for Indonesia's forest fires. *Conserv Biol* 30:5–6.
12. The World Bank (2016) *The Cost of Fire: An Economic Analysis of Indonesia's 2015 Fire Crisis* (World Bank Group, Jakarta, Indonesia).
13. Tacconi L (2016) Preventing fires and haze in Southeast Asia. *Nat Clim Chang* 6: 640–643.
14. Field RD, van der Werf GR, Shen SS (2009) Human amplification of drought-induced biomass burning in Indonesia since 1960. *Nat Geosci* 2:185–188.
15. Miettinen J, Shi C, Liew SC (2016) Land cover distribution in the peatlands of Peninsular Malaysia, Sumatra and Borneo in 2015 with changes since 1990. *Glob Ecol Conserv* 6:67–78.
16. Warren M, Hergoualc'h K, Kauffman JB, Murdiyarso D, Kolka R (2017) An appraisal of Indonesia's immense peat carbon stock using national peatland maps: Uncertainties and potential losses from conversion. *Carbon Balance Manag* 12:12.
17. Page SE, Rieley JO, Banks CJ (2011) Global and regional importance of the tropical peatland carbon pool. *Glob Chang Biol* 17:798–818.
18. Page SE, Hooijer A (2016) In the line of fire: The peatlands of Southeast Asia. *Philos Trans R Soc Lond B Biol Sci* 371:20150176.
19. Konecny K, et al. (2016) Variable carbon losses from recurrent fires in drained tropical peatlands. *Glob Chang Biol* 22:1469–1480.
20. Miettinen J, Hooijer A, Vernimmen R, Liew SC, Page SE (2017) From carbon sink to carbon source: Extensive peat oxidation in insular Southeast Asia since 1990. *Environ Res Lett* 12:024014.
21. Usup A, Yoshihiro H, Takahashi H, Hayasaka H (2004) Combustion and thermal characteristics of peat fire in tropical peatland in Central Kalimantan, Indonesia. *Tropics* 14:1–19.
22. Huang X, Restuccia F, Gramola M, Rein G (2016) Experimental study of the formation and collapse of an overhang in the lateral spread of smouldering peat fires. *Combust Flame* 168:393–402.
23. Wooster MJ, et al. (2018) New tropical peatland gas and particulate emissions factors indicate 2015 Indonesian fires released far more particulate matter (but less methane) than current inventories imply. *Remote Sens* 10:495.
24. Jayarathne T, et al. (2018) Chemical characterization of fine particulate matter emitted by peat fires in Central Kalimantan, Indonesia, during the 2015 El Niño. *Atmos Chem Phys* 18:2585–2600.
25. Stockwell CE, et al. (2016) Field measurements of trace gases and aerosols emitted by peat fires in Central Kalimantan, Indonesia, during the 2015 El Niño. *Atmos Chem Phys* 16:11711–11732.
26. Akagi S, et al. (2011) Emission factors for open and domestic biomass burning for use in atmospheric models. *Atmos Chem Phys* 11:4039–4072.
27. Turetsky MR, et al. (2015) Global vulnerability of peatlands to fire and carbon loss. *Nat Geosci* 8:11–14.
28. Dommain R, Couwenberg J, Glaser PH, Joosten H, Suryadiputra INN (2014) Carbon storage and release in Indonesian peatlands since the last deglaciation. *Quat Sci Rev* 97:1–32.
29. Marlier ME, et al. (2015) Regional air quality impacts of future fire emissions in Sumatra and Kalimantan. *Environ Res Lett* 10:054010.
30. Miettinen J, Shi C, Liew SC (2017) Fire distribution in Peninsular Malaysia, Sumatra and Borneo in 2015 with special emphasis on peatland fires. *Environ Manage* 60: 747–757.

31. van der Werf GR, et al. (2017) Global fire emissions estimates during 1997–2016. *Earth Syst Sci Data* 9:697–720.
32. Levin I, Hesshaimer V (2000) Radiocarbon: A unique tracer of global carbon cycle dynamics. *Radiocarbon* 42:69–80.
33. Trumbore S (2000) Age of soil organic matter and soil respiration: Radiocarbon constraints on belowground C dynamics. *Ecol Appl* 10:399–411.
34. Mouteva G, et al. (2015) Black carbon aerosol dynamics and isotopic composition in Alaska linked with boreal fire emissions and depth of burn in organic soils. *Global Biogeochem Cycles* 29:1977–2000.
35. Page S, et al. (2004) A record of late pleistocene and Holocene carbon accumulation and climate change from an equatorial peat bog (Kalimantan, Indonesia): Implications for past, present and future carbon dynamics. *J Quat Sci* 19:625–635.
36. Stuiver M, Polach HA (1977) Discussion reporting of ^{14}C data. *Radiocarbon* 19: 355–363.
37. Supiandi S, Furukawa H (1986) A study of floral composition of peat soil in the lower batang hari river basin of Jambi, Sumatra. *South Asian Stud* 24:113–132.
38. Maloney B, McCormac F (1995) A 30,000-year pollen and radiocarbon record from highland Sumatra as evidence for climatic change. *Radiocarbon* 37:181–190.
39. Page SE, Rieley JO, Shotyk W, Weiss D (1999) Interdependence of peat and vegetation in a tropical peat swamp forest. *Philos Trans R Soc Lond B Biol Sci* 354:1885–1897.
40. Wüst RA, Jacobsen GE, von der Gaast H, Smith AM (2008) Comparison of radiocarbon ages from different organic fractions in tropical peat cores: Insights from Kalimantan, Indonesia. *Radiocarbon* 50:359–372.
41. Gandois L, et al. (2014) Origin, composition, and transformation of dissolved organic matter in tropical peatlands. *Geochim Cosmochim Acta* 137:35–47.
42. Biagioni S, et al. (2015) 8000 years of vegetation dynamics and environmental changes of a unique inland peat ecosystem of the Jambi province in central Sumatra, Indonesia. *Palaeogeogr Palaeoclimatol Palaeoecol* 440:813–829.
43. Cobb AR, et al. (2017) How temporal patterns in rainfall determine the geomorphology and carbon fluxes of tropical peatlands. *Proc Natl Acad Sci USA* 114: E5187–E5196.
44. Hu S, Fedorov AV (2016) Exceptionally strong easterly wind burst stalling El Niño of 2014. *Proc Natl Acad Sci USA* 113:2005–2010.
45. Pataki D, Bowling D, Ehleringer J (2003) Seasonal cycle of carbon dioxide and its isotopic composition in an urban atmosphere: Anthropogenic and biogenic effects. *J Geophys Res D Atmos,* 108:4735.
46. Hua Q, Barbetti M, Rakowski AZ (2013) Atmospheric radiocarbon for the period 1950–2010. *Radiocarbon* 55:2059–2072.
47. Ismail A, Mamat MN (2002) The optimal age of oil palm replanting. *Oil Palm Ind Econ J* 2:11–18.
48. Tan KP, Kanniah KD, Cracknell AP (2013) Use of UK-DMC 2 and ALOS PALSAR for studying the age of oil palm trees in southern peninsular Malaysia. *Int J Remote Sens* 34:7424–7446.
49. Kurokawa H, Yoshida T, Nakamura T, Lai J, Nakashizuka T (2003) The age of tropical rain-forest canopy species, Borneo ironwood (Eusideroxylon zwageri), determined by ^{14}C dating. *J Trop Ecol* 19:1–7.
50. Yoneda T, Tamin R, Ogino K (1990) Dynamics of aboveground big woody organs in a foothill dipterocarp forest, West Sumatra, Indonesia. *Ecol Res* 5:111–130.
51. Dommain R, Couwenberg J, Joosten H (2011) Development and carbon sequestration of tropical peat domes in South-east Asia: Links to post-glacial sea-level changes and Holocene climate variability. *Quat Sci Rev* 30:999–1010.
52. Anderson J, Muller J (1975) Palynological study of a Holocene peat and a Miocene coal deposit from NW Borneo. *Rev Palaeobot Palynol* 19:291–351.
53. Yulianto E, Hirakawa K, Tsuji H (2004) Charcoal and organic geochemical properties as an evidence of Holocene fires in tropical peatland, Central Kalimantan, Indonesia. *Tropics* 14:55–63.
54. Diemont W, Supardi (1987) Accumulation of organic matter and inorganic constituents in a peat dome in Sumatra, Indonesia. *International Peat Society Symposium on Tropical Peat and Peatlands for Development* (International Peat Society, Yogyakarta, Indonesia), pp 698–708.
55. Murdiyarso D, Hergoualc'h K, Verchot LV (2010) Opportunities for reducing greenhouse gas emissions in tropical peatlands. *Proc Natl Acad Sci USA* 107:19655–19660.
56. van der Werf GR, et al. (2008) Climate regulation of fire emissions and deforestation in equatorial Asia. *Proc Natl Acad Sci USA* 105:20350–20355.
57. Reimer PJ, et al. (2013) IntCal13 and Marine13 radiocarbon age calibration curves 0–50,000 years cal BP. *Radiocarbon* 55:1869–1887.
58. Giglio L, Descloitres J, Justice CO, Kaufman YJ (2003) An enhanced contextual fire detection algorithm for MODIS. *Remote Sens Environ* 87:273–282.
59. Park RJ, Jacob DJ, Field BD, Yantosca RM, Chin M (2004) Natural and transboundary pollution influences on sulfate-nitrate-ammonium aerosols in the United States: Implications for policy. *J Geophys Res D Atmos,* 109:D15204.
60. Keller CA, et al. (2014) HEMCO v1. 0: A versatile, ESMF-compliant component for calculating emissions in atmospheric models. *Geosci Model Dev* 7:1409–1417.